Confirmation of the Solution Structure of Tyrocidine A using Perturbation of Proton Relaxation Rates by Nitroxide Spin Labels

Ning Zhou
Department of Biochemistry, University of Wisconsin, Madison, Wisconsin 53706, U.S.A.
Paolo Mascagni and William A. Gibbons *
Department of Pharmaceutical Chemistry, School of Pharmacy, University of London, 29/39 Brunswick Square, London WC1N 1AX
Neri Niccolai and Claudio Rossi
Department of Chemistry, University of Siena, Siena, Italy
Herman Wyssbrod
Department of Physiology and Biophysics, Mount Sinai School of Medicine, New York, U.S.A.

The spin–lattice relaxation rate enhancements of the protons of tyrocidine A upon addition of 2,2,6,6-tetramethylpiperidin-1-oxyl (TEMPO) were analysed in solution and were shown to be consistent with the peptide conformation. The effects on tyrocidine A proton spin–lattice relaxation rates for three TEMPO derivatives in two different solvents have also been studied in order to obtain information about the influence of TEMPO substituents on nitroxide–biomolecule interactions. The neutral free radical TEMPO exhibits less specificity in its interaction with tyrocidine A than its derivatives and, hence, it is the most suitable probe for generally investigating conformational moieties of biomolecules in solution. By corollary, charged nitroxides should be probes of the microenvironment surrounding the specific site of interaction.

It has recently been shown that stable, neutral, soluble nitroxide free radicals such as 2,2,6,6-tetramethylpiperidin-1-oxyl (TEMPO) can be used to delineate solvent-shielded *versus* solvent-exposed protons of complex molecules.[1–3] This was achieved by analysing the perturbations induced by these paramagnetic species on the proton relaxation rates of biopolymers. The relative rate enhancements were found to be dominated by molecular conformation, since outer protons, in general, have the largest relaxation rate enhancement. These findings were qualitatively interpreted in terms of dipolar interactions between the electronic spin, S, of the unpaired electron of the nitroxide, and the nuclear spins, I, of protons attached to the biomolecule.[4,5]

Here we compare the interaction of four nitroxides containing the polar hydroxy, carboylic acid moieties, and the positive choline group with tyrocidine A, which contains a variety of amino acid side-chains and three different conformational moieties: the β sheet, β II′ and β I turns (Figure 1).

Experimental

The tyrocidine A was obtained from the late Professor L. C. Craig and was purified by counter-current distribution. After lyophilizing, tyrocidine A was dissolved in 100% [$^2H_6$]DMSO and 99.9% CD_3OD (Aldrich). 2,2,6,6-Tetramethylpiperidin-1-oxyl (TEMPO) (**1**), 2,2,6,6-tetramethyl-4-hydroxypiperidin-1-oxyl (**2**) (TEMPOL), *N*-(2-hydroxyethyl)-*NN*-dimethyl-*N*-(1-oxyl-2,2,6,6-tetramethylpiperidin-4-yl)-ammonium chloride (TEMPOCHOLINE) and 1-oxyl-2,2,5,5-tetramethyl-3-pyrroline-3-carboxylic acid (**4**) (TEMPIC ACID) were obtained from Aldrich, Molecular Probes, and Eastman Kodak, respectively. Stock solutions were mixed with solutions of the peptide to yield samples of known concentrations. The n.m.r. spectra were recorded with a Bruker WH 270 instrument interfaced with a Nicolet 1180 computer.

Spin–lattice relaxation rates were measured from partially relaxed spectra (Figure 2), obtained using a $(180°–\tau–90°–T)_n$ pulse sequence. Relaxation rates were calculated from semi-log plots of $(M_0 - M_\tau)/2M_0$ *versus* τ; a ± 5% experimental error

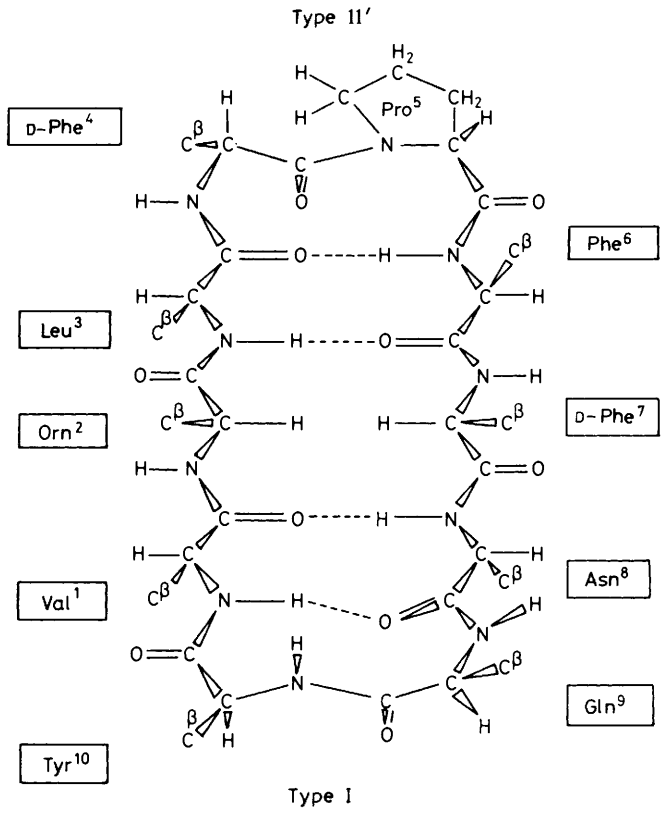

Figure 1. Tyrocidine A secondary structure according to refs. 5 and 6

was estimated. Reported values of S_{1p}, the nitroxide molar enhancement of relaxation rates per mole of tyrocidine A, were calculated according to relationships (1) and (2) where R_1 is the

$$R_{1\text{exp.}} - R_1 = R_{1p} \quad (1)$$

$$S_{1p}' = R_{1p}/[\text{SL}];\ S_{1p} = S_{1p}'/[\text{Tyr}] \quad (2)$$

relaxation rate measured in the absence of nitroxides and R_{1exp} is the same rate but measured in the presence of different concentrations of nitroxide, [SL]. The peptide concentration, [Tyr], was maintained constant at 20 mM for experiments in [$^2H_6$]DMSO solutions and 15 mM in CD_3OD solutions, while [SL] ranged between 5 and 50 mM. Figure 3 shows a typical S_{1p}' calculation. The estimated average accuracy of S_{1p} was ± 10%.

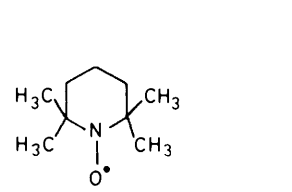

(1)

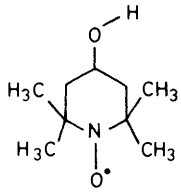

(2)

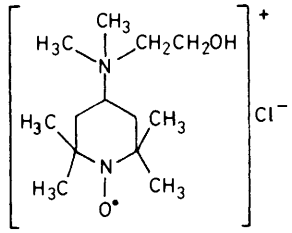

(3)

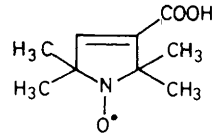

(4)

Results and Discussion

The backbone structure and most of the side-chain conformations of tyrocidine A in solution have been elucidated by using interproton distances derived from NOE,[6] proton relaxation,[7] and scalar coupling[8,9] parameters. A preliminary study of the relative enhancements of proton relaxation rates induced by TEMPO nitroxide has been reported;[2] it was concluded that, as in the case of gramicidin S,[1] these enhancements were determined by the relative solvent exposure of the individual protons and hence by the conformation. This approach, therefore, has been proposed as a criterion for conformational moieties in peptides, especially for intramolecular hydrogen bonds, and is more generally useful and easier to quantitate than linewidth measurements.[3]

1. *The effect of the Nitroxide Free Radical TEMPO on the Spin–Lattice Relaxation Rates of the Protons of Tyrocidine A.*— Figure 4 shows the effect of the nitroxide radical TEMPO on the 270 MHz tyrocidine A ^1H n.m.r. spectrum in $(CD_3)_2SO$. Using the experimental conditions described in the caption to Figure 4, neither significant line broadening nor chemical shift changes were observed. On the other hand, this concentration of TEMPO produced large and accurately measurable enhancements of the non-selective relaxation rates of all amide and side-chain protons, as seen in Figure 2. This effect is similar to that reported for gramicidin S.[1] Semilogarithmic plots of peak area *versus* τ yielded the ^1H relaxation rates, R_1, of (a) most classes of protons and (b) many individual protons in tyrocidine A. These rates were determined as a function of TEMPO concentration. R_{1p}, and S_{1p}' are shown in the Table.

Backbone proton relaxation enhancements and conformation. Because of spectral overlap at δ 7.2, no data were obtained for Phe[6] NH, but the enhancements of the other amide protons are

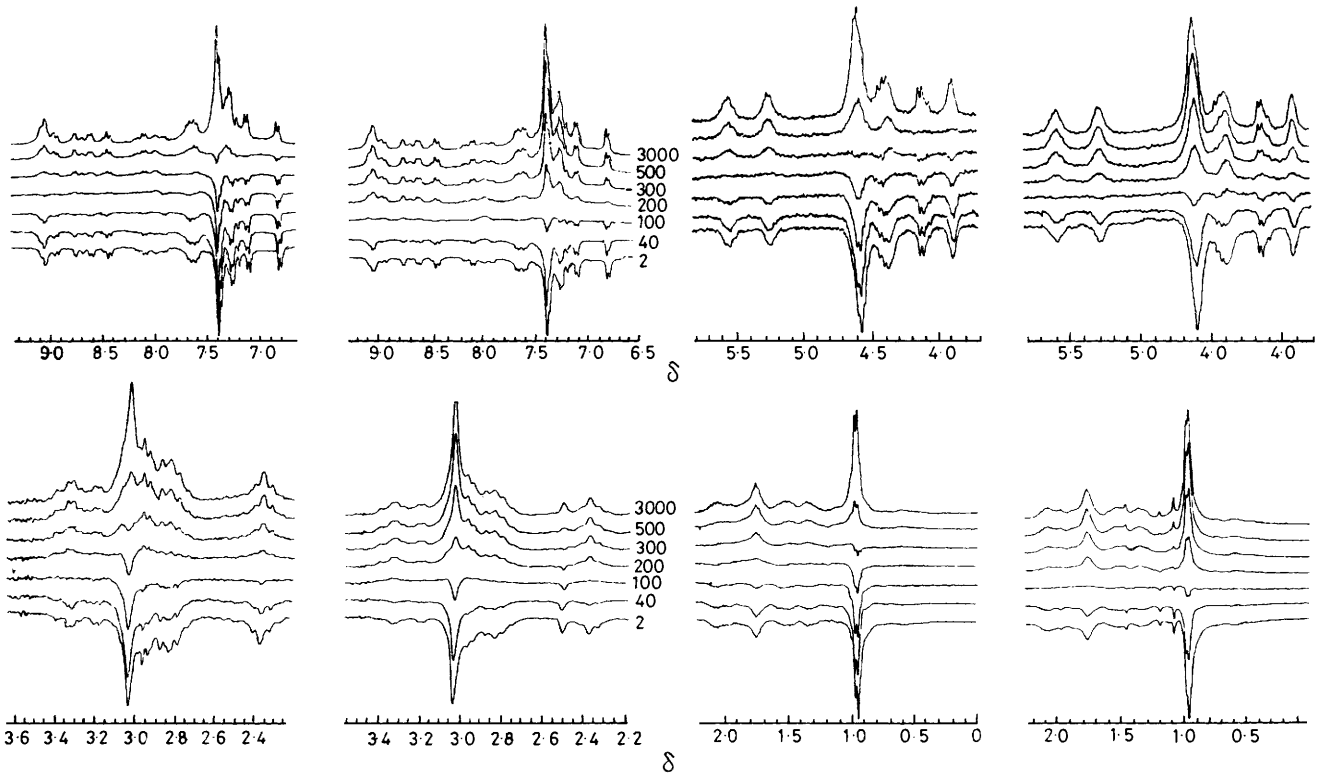

Figure 2. Partially recovered ^1H n.m.r. spectra of selected regions for tyrocidine A studied under the same experimental conditions reported in the caption to Figure 4. The spectra on the right of each pair reflect the effects of 38.4mM-TEMPO. All sequences refer to identical recovery time (τ); values from top to bottom are 3 000, 500, 300, 200, 100, 40, and 2 ms

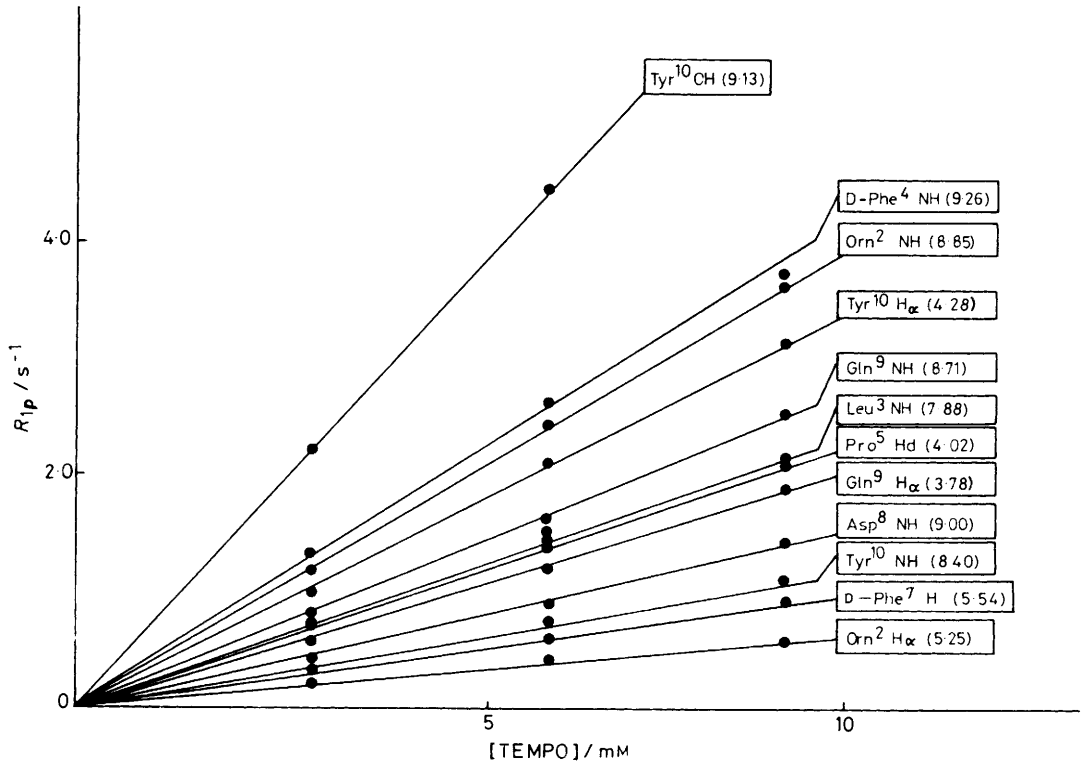

Figure 3. R_{1p} dependence observed for some tyrocidine A protons upon additions of TEMPO. S_{1p} values were calculated from R_{1p} *versus* TEMPOL slopes. Peptide concentration was 20mM in [$^2H_6$]DMSO. Values in parenthesis represent proton chemical shift in p.p.m. from internal Me_4Si

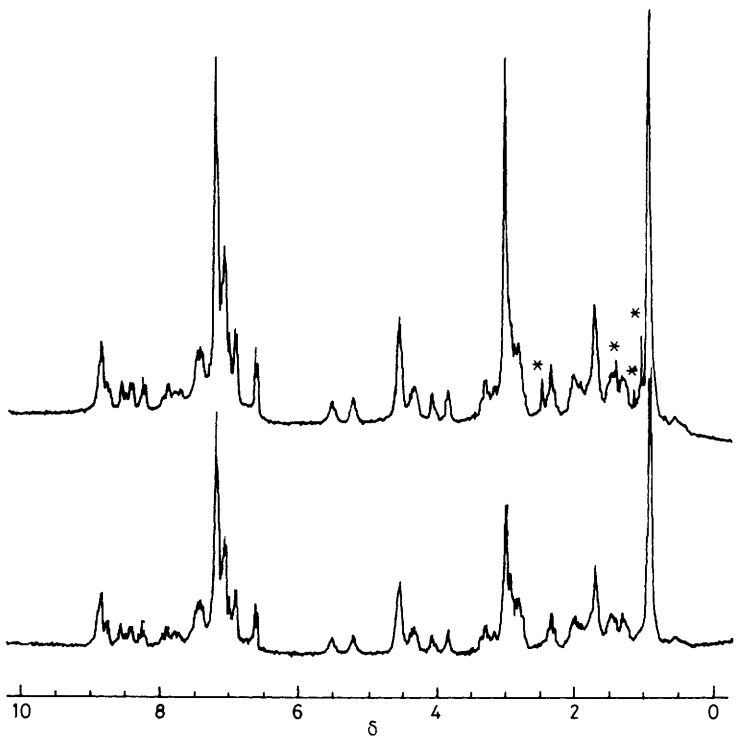

Figure 4. 270 MHz ^1H N.m.r. spectrum of tyrocidine A (24mM) in $(CD_3)_2SO$ at 77 °C. Bottom: in absence of TEMPO; top: in presence of 38.4mM-TEMPO. Lines marked with * are from TEMPO

Effect of the nitroxide TEMPO on proton relaxation rates: comparison with amide proton exchange rates and temperature coefficients of chemical shifts

Proton	Chemical shift[a] (p.p.m.)	Relaxation rate for a given concentration of nitroxide R_1/s^{-1} TEMPO (mM) 0	12.8	38.4	S_{1p}'/s^{-1} mol^{-1} l	$\Delta\delta_{NH}/\Delta T$ (p.p.b./°C)	$10^6 k_{HDX}/s^{-1}$
D-Phe^4 NH	9.26	3.1	4.4	6.4	90	−6.5	>3 000
D-Phe^7 NH	9.01	3.8	5.1	8.3	115	−4.6	
Asn^8 NH	9.00	3.7	4.4	5.7	52	−3.0	~15
Orn^2 NH	8.85	3.9	5.5	8.6	122	−7.4	~50
Gln^9 NH	8.71	4.7	6.3	9.6	125	−3.1	~55
Tyr^{10} NH	8.40	4.4	4.9	5.7	36	−3.1	~5
Leu^3 NH	7.88	4.2	5.0	6.2	54	0	~3.5
Val^1 NH	7.39	2.8	3.5	4.8	52	−1.2	~2
D-Phe^7 α[a]	5.55	3.4	3.7	4.4	26		
Orn^2 α	5.26	3.3	3.8	4.9	43		
Val^1 α[b]	4.52	2.3	3.5	5.8	94		
Leu^3 α[b]	4.51	2.3	3.5	5.8	94		
Asn^8 α[b]	4.46	2.3	3.5	5.8	94		
Phe^6 α[b]	4.45	2.3	3.5	5.8	94		
Tyr^{10} α	4.28	2.1	2.9	4.6	64		
D-Phe^4 α	4.23	2.9	4.6	8.2	132		
Pro^5 α	4.03	1.7	2.5	4.3	68		
Gln^9 α	3.78	1.6	2.4	4.1	63		
Tyr^{10} OH	~9.1	2.6	3.7	6.2	86		
Phe Arom CH[c]	~7.2	1.3	2.5	5.0	94		
Tyr^{10} *m*-Arom CH	6.89	1.4	2.3	4.4	70		
Tyr^{10} *o*-Arom CH	6.59	1.0	1.9	4.0	70		
Pro^5 δD[d]	3.26	6.1	7.6	10.2	117		
Asn^8 β[d]	~3.2	6.3	7.7	10.7	109		
Tyr^{10} β[d]	2.90	5.3	6.9	9.9	125		
D-Phe^7 β[d]	~2.8	5.3	6.9	9.9	125		
Orn^2 δ[d]	2.75	4.3	5.8	8.7	117		
Phe^6 β[d]	~2.2	5.8	6.9	9.2	86		
Pro^5 δU[d]	2.13	5.8	6.9	9.2	86		
Val^1 β[d]	1.97	2.5	3.5	5.5	78		
Orn^2 β[d]	~1.7	3.9	4.9	6.9	78		
Orn^2 γ[d]	1.64	5.3	6.3	8.2	78		
Gln^9 β[d]	1.61	5.3	6.3	8.2	78		
Leu^3 γ[d]	1.43	2.8	4.3	6.3	104		
Pro^5 βD[d]	1.42	3.5	5.0	6.9	103		
Leu^3 β[d]	~1.3	3.5	5.0	6.9	103		
Pro^5 βU[d]	1.10	3.5	5.0	6.9	103		
Leu^3 δ[d]	~0.9	2.0	3.2	5.5	86		
Val^1 γ[d]	0.87	2.5	3.5	5.5	78		
Pro^5 γU[d]	0.33	3.5	4.7	6.9	86		

[a] Ref. 7. [b] These relaxation rates were calculated as a mean for all four unresolved α proton multiples. [c] D-Phe^4, Phe^6, and D-Phe^7. [d] Because of overlapping proton resonances, these values are less accurate than others in this table; these numbers were estimated from the null point: $R_1 = \ln 2/\tau_{null}$.

fully consistent with the proposed structure. The small relative enhancements (S_{1p}' 52—54 s^{-1} mol^{-1} l) for Val^1 NH, Leu^3 NH, and Asn^8 NH correspond to inner-pointing, hydrogen-bonded amide protons of the antiparallel β-pleated sheet moiety, whereas the large relative enhancements (S_{1p}' 90—125 s^{-1} mol^{-1} l) for Orn^2 NH, D-Phe^4 NH, D-Phe^7 NH, and Gln^9 NH correspond to outer-pointing, solvent-exposed amide protons. Although Tyr^{10} NH is axial to the backbone ring in the type I β-turn, its relatively low S_{1p}' value (36 s^{-1} mol^{-1} l) suggests that it is either sterically shielded from solvent by the side-chains of Gln^9 and Tyr^{10} or involved in the formation of a hydrogen bond with a side-chain.

The S_{1p}' values for all protons are also consistent with the conformation shown in Figure 1; the characteristics of the enhancements of these protons are similar to those of the amide protons, *i.e.*, the equatorial innerpointing protons, Orn^2 H_α and D-Phe^7 H_α, have low S_{1p}' values (43 and 26 s^{-1} mol^{-1} l, respectively), and the protons of the other eight residues (residues 1, 3—6, and 8—10), being relatively more exposed to solvent, have S_{1p}' values of 63—132 s^{-1} mol^{-1} l.

Side-chain proton relaxation enhancements and conformation. Because of spectral overlap accurate S_{1p}' values were not obtained for all of the side-chain protons. Generally these protons were characterized by large S_{1p} values in the range from 70 to 125 s^{-1} mol^{-1} l, consistent with their being exposed to solvent to a greater extent than the shielded backbone protons characterized by values from 52 to 54 s^{-1} mol^{-1} l.

Criteria for hydrogen bonds. Not only are the S_{1p}' data consistent with the proposed conformation of tyrocidine A, thereby indicating that the determining factor in relative S_{1p}' values is indeed the peptide conformation, but they also provide criteria for β-pleated sheet structures, β-turns, and perhaps other conformations. To demonstrate that our proposed S_{1p} criteria for hydrogen bonds are valid, S_{1p}' was plotted against

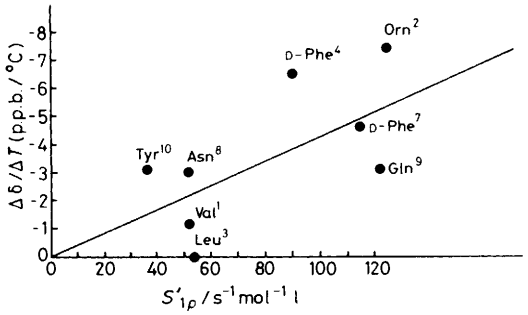

Figure 5. Temperature coefficient of amide proton chemical shifts ($\Delta\delta/\Delta T$) *versus* nitroxide-induced relaxation enhancement per unit concentration of added TEMPO (S_{1p}')

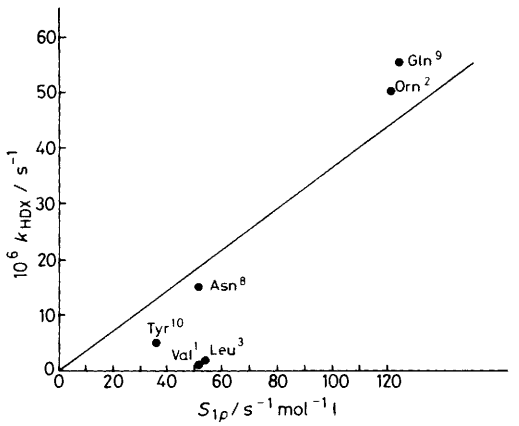

Figure 6. Exchange rate of amide protons (k_{HDX}) *versus* nitroxide-induced relaxation rate enhancement per unit concentration of added TEMPO (S_{1p}')

two commonly used criteria, $\Delta\delta/\Delta T$, the temperature coefficient of the amide proton chemical shift (Figure 5), and k_{HDX}, the amide proton–deuteron exchange rate (Figure 6). The value of the product-moment correlation coefficient, r, for the paired values of $\Delta\delta/\Delta T$ and S_{1p}' shown in Figure 5 is 0.6307 (ν = degrees of freedom = 6), and the value of r for the paired values of k_{HDX} and S_{1p}' shown in Figure 6 is 0.9713 (ν = 4). The hypothesis that there is no correlation between the values can be rejected at the 0.094 level of significance for the former set of values and at the 0.0012 level for the latter set. These correlations are consistent with the proposal that nitroxide perturbations of linewidths[3] and relaxation rates[1] provide simple criteria for determining the relative exposures of amide protons to solvent, which can, in turn, be related to whether these protons are involved in the formation of intramolecular hydrogen bonds.

2. *The Effect of Nitroxide Charge and Polarity on Nitroxide–Peptide Interactions: the Use of Correlation Diagrams.*—The details of the interaction of neutral TEMPO with tyrocidine A have been elucidated and hence the use of S_{1p} correlation diagrams such as Figures 7 and 8 are effective means of deducing the role of nitroxide substitution and solvent polarity on the relative relaxation enhancements.

The first obvious conclusion from the diagrams is that no matter what the nature of the substituent an inherent first-order correlation exists. Substituent effects therefore result in (a) an increased generalized interaction of each nitroxide over and above that of TEMPO and (b) specific effects due to specific yet

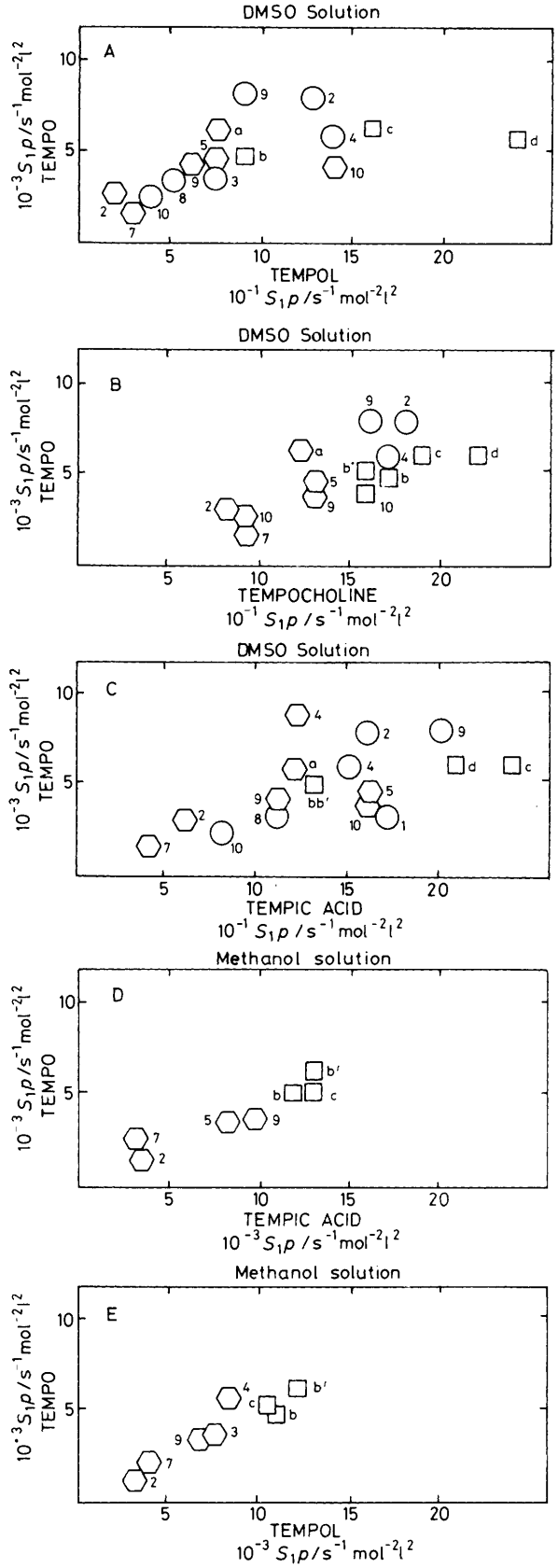

Figure 7. Nitroxide–nitroxide S_{1p} correlation diagrams of DMSO solution (A, B, C) and of methanol solutions (D, E). ◯, amide protons; ⬡, H_α; numbers indicate the residue. [b] and [b'] refer to $Tyr^{10}H_\delta$ and H_ϵ respectively; [c] = Phe aromatic side-chains; [d] = Tyr^{10} aromatic proton; ⟨a⟩ = Val^1, Leu^3, Phe^6, Asn^8 H_α

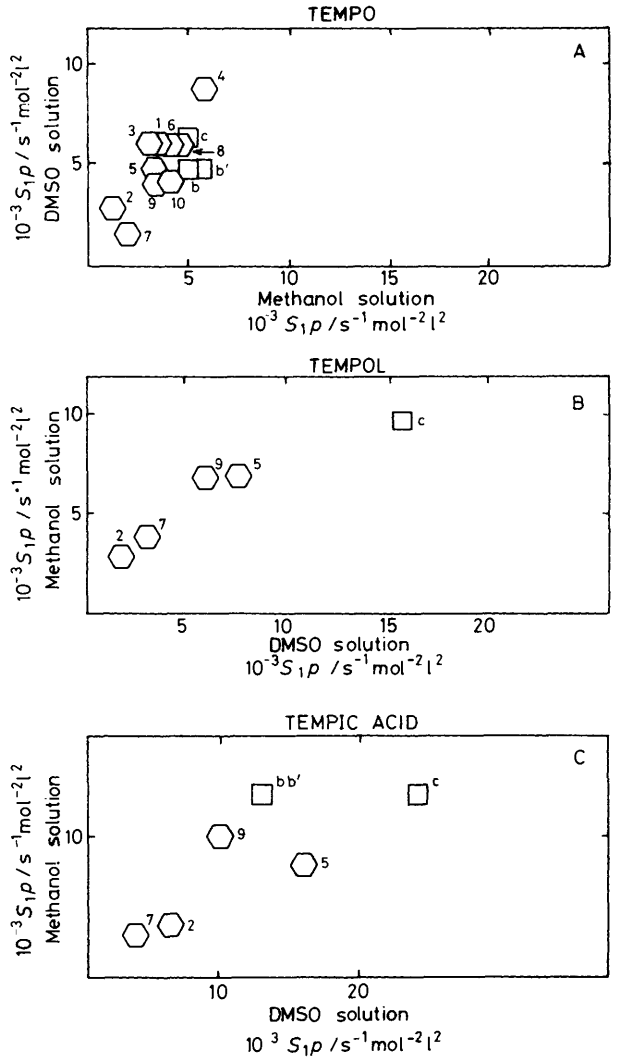

Figure 8. DMSO–Methanol S_{1p} correlation diagrams of TEMPO (A), TEMPOL (B), and TEMPIC ACID (C) nitroxides. ⬡ = H_α; numbers indicate the residue. [b] and [b'] refer to Tyr^{10} H_δ and H_ε respectively; [c] = Phe aromatic side-chains

weak complexes between the nitroxide substituent and the side-chain and backbone groups on tyrocidine.

Examples of these two features are readily seen: (a) solvent-shielded backbone protons (Orn^2H_α, D-Phe^7H_α, Asn^8NH, Phe^6NH, Leu^3NH, Val^1NH, and $Tyr^{10}NH$) exhibit the smallest S_{1p} enhancements whereas external protons such as Tyr^{10} ring protons, Orn^2NH, and Phe^4NH exhibit large S_{1p} enhancements, (b) the TEMPIC ACID COOH group specifically interacts with the βI turn residues Asn^8-Glu^9-Tyr^{10}-Val^1 as shown by the relatively large S_{1p} values for Glu^9NH, Val^1NH, $Tyr^{10}H_\alpha$, and Tyr^{10} ring protons in Figure 7C. This can be attributed to hydrogen bonding between the COOH group and one of the carboxamide or phenolic OH groups, (c) the very large enhancements of $Tyr^{10}H_\alpha$ and Tyr^{10} ring protons with TEMPOL (Figure 7A) are consistent with more specific complexation within the vicinity of the Tyr^{10} residue, (d) apart from an increased generalized interaction, TEMPOCHOLINE (Figure 7B) shows no specific interaction with any of the groups of tyrocidine A.

Quantitative interpretation of these findings is difficult since it necessitates a knowledge of (a) the strengths of the relative interactions of nitroxide–solvent and nitroxide–peptide, (b) the mode(s) of interaction that govern nitroxide–peptide general interactions, and (c) the mechanisms of proton relaxation enhancement. Qualitatively, however, the increased strength of the generalized interaction with substituted nitroxides could be due to (a) the relative decrease in solvent–nitroxide interactions on substitution of the nitroxide, (b) the concomitant increased strengths of complexes of nitroxides with the peptide groups on tyrocidine *via* hydrogen bonds and/or the random collisional complexes between nitroxide and peptide. Both of these are fully consistent with the modes of interaction elucidated for solvent–nitroxide mixtures.[5,10]

3. *Solvent Effects on Nitroxide–Tyrocidine A Interactions.*—Three main aspects can, in principle, be analysed by solvent-dependence studies of the S_{1p} values: (a) the role of different solvent–nitroxide complexation on the nitroxide–biomolecule interaction; (b) how S_{1p} values can reflect solvent-induced conformational change; (c) the existence of solvents which are more advantageous than others for performing nitroxide perturbation studies of proton relaxation rates.

The effects of different solvents on the dynamics and structural features involved in the nitroxide–tyrocidine A interaction can be visualized using correlation diagrams similar to those previously discussed.

Since in DMSO and methanol the secondary structure of the decapeptide is unchanged,[7] the interpretation of the correlation diagrams, in Figure 8, for these two solvents should provide information on the nitroxide–tyrocidine systems.

From solvent correlation diagrams of TEMPOL and TEMPIC ACID, Figures 8B and C, respectively, it is possible to argue that these two nitroxides act similarly in these two solvents. TEMPO behaves differently since, on average, it yields higher S_{1p} values in DMSO than in methanol solutions. These findings can be explained on the basis of different solvation of the three nitroxides. Thus TEMPOL and TEMPIC ACID form, with both solvents, complexes of comparable stabilities, while TEMPO is more solvated when dissolved in methanol solutions and, hence, less available to tyrocidine A external protons.

Conclusions.—Neutral, hydroxylated, protonated, and carboxylic acid-substituted nitroxides have been used to enhance proton spin–lattice relaxation rates of tyrocidine A in methanol and DMSO solutions. As previously observed using TEMPO and gramicidin S[1] the relaxation enhancements for tyrocidine A are mainly controlled by the peptide conformation. Correlation diagrams were utilized to gain detailed information on the nature of nitroxide–tyrocidine interaction. The relative relaxation enhancements of the backbone H and NH protons are fully consistent with tyrocidine A possessing a β-pleated sheet, βI turn, and βII′ turn conformational moieties. Several aspects of the side-chain conformations were also confirmed but, since R_1 values could not be measured for most specific side-chain protons because of spectral overlap, this area could not be further explored.

The fact that, in general, TEMPO, the neutral nitroxide, causes the smallest effects on proton relaxation rates of tyrocidine A can be ascribed to (a) additional specific interactions between TEMPOL, TEMPOCHOLINE, TEMPIC ACID, and the peptide or (b) less elastic random collisions, since the latter three nitroxides deviate more than TEMPO from the model of chemically inert spheres. In both cases, therefore, TEMPO is a more suitable probe for detecting conformational moieties than the substituted nitroxides. Furthermore, TEMPO induces paramagnetic perturbations whose extent depends also on the stability of its complexes with the solvent. It should be noted that the formation of highly stable nitroxide–solvent complexes has to be avoided since it favours long-range free radical-

biomolecule interactions which are associated to less specific paramagnetic relaxation contributions. In fact, these 'outer sphere' dipolar relaxation contributions have a looser dependence on the electron–nucleus distance of approach[11] than the 'inner sphere' ones.[12] However, with large molecules, the existence of nitroxides that would specifically complex with (say) a given class of side-chain could be of considerable use as a specific probe and for n.m.r. assignments.

Acknowledgements

This work was partly supported by grants from N.S.F. (PCM 7911568), N.I.H. (AM 18604), by the Searle Family Trust, and by grants from the Italian C.N.R.

References

1 N. Niccolai, G. Valensin, C. Rossi, and W. A. Gibbons, *J. Am. Chem. Soc.*, 1982, **104**, 1534.
2 N. Niccolai, N. Zhou, C. Rossi, P. Mascagni, and W. A. Gibbons, Proc. 7th Am. Peptide Symposium, eds D. H. Rich and E. Gross, Pierce Chemical Co., Rockford, Illinios, 1981, p. 307.
3 K. D. Kopple and T. J. Schamper, *J. Am. Chem. Soc.*, 1977, **99**, 7698.
4 N. Niccolai, C. Rossi, G. Valensin, P. Mascagni, and W. A. Gibbons, *J. Phys. Chem.*, 1984, **88**, 5689.
5 Z. W. Qui, D. M. Grant, and R. J. Pugmire, *J. Am. Chem. Soc.*, 1982, **104**, 2747.
6 M. C. Kuo and W. A. Gibbons, *Biophys. J.*, 1980, **32**, 807.
7 M. C. Kuo, T. Drakenberg, and W. A. Gibbons, *J. Am. Chem. Soc.*, 1980, **102**, 520.
8 M. C. Kuo and W. A. Gibbons, *Biochemistry*, 1979, **18**, 5855.
9 M. C. Kuo, PhD Thesis, University of Wisconsin-Madison, 1980.
10 H. W. Nientiedt, K. Kundfuss, and W. Muller-Warmuth, *J. Magn. Reson.*, 1981, **43**, 154.
11 P. S. Hubbard, *Proc. R. Soc. London*, 1966, **A29**, 537.
12 N. Bloembergen and L. D. Morgan, *J. Chem. Phys.*, 1961, **34**, 842.

Received 11*th July* 1984; *Paper* 4/1202